



# CHORUS

This is the accepted manuscript made available via CHORUS. The article has been published as:

## Macroscopic magnetic structures with balanced gain and loss

J. M. Lee, T. Kottos, and B. Shapiro

Phys. Rev. B **91**, 094416 — Published 17 March 2015

DOI: [10.1103/PhysRevB.91.094416](https://doi.org/10.1103/PhysRevB.91.094416)

# Macroscopic magnetic structures with balanced gain and loss

J. M. Lee, T. Kottos

*Department of Physics, Wesleyan University, Middletown, Connecticut 06459*

B. Shapiro

*Technion - Israel Institute of Technology, Technion City, Haifa 32000, Israel*

(Dated: March 4, 2015)

We investigate magnetic nanostructures with balanced gain and loss and show that such configurations can result in a new type of dynamics for magnetization. Using the simplest possible set-up consisting of two coupled ferromagnetic films, one with loss and another one with a balanced amount of gain, we demonstrate the existence of an exceptional point where both the eigenfrequencies and eigenvectors become degenerate. This point corresponds to a particular value of gain and loss parameter  $\alpha = \alpha_c$ . For  $\alpha < \alpha_c$  the frequency spectrum is real, indicating stable dynamics, while for  $\alpha > \alpha_c$  it is complex, signaling unstable dynamics which is, however, stabilized by nonlinearity.

PACS numbers: 11.30.Er, 76.50.+g, 05.45.Xt,

## I. INTRODUCTION

Spin dynamics in synthetic magnetic nanostructures has attracted increasing attention during the last years<sup>1</sup>, because of the interesting fundamental physics involved and also due to its important practical applications: magnetic storage and information processing<sup>2,3</sup>, sensing<sup>4</sup>, and creation of tunable high frequency oscillators<sup>5</sup> are some of the areas that have been benefited by this research activity. An important step in this endeavor is the realization of new magnetic nanodevice architectures with additional degrees of freedom which permit better control of magnetization dynamics.

Along the same lines, management of classical wave propagation via synthetic structures has been proven to be successful resulting in the creation of new materials with unexpected properties. Examples of this success include the realization of meta-materials which exhibit phenomena like cloaking, negative index of refraction, etc. The operation frequency for many of these proposals spans a wide range from optics<sup>6</sup> and micro-waves<sup>7</sup> to acoustics<sup>8</sup>. Quite recently, a new type of synthetic structures which possesses spatio-temporal reflection symmetry, or parity-time ( $\mathcal{PT}$ ) symmetry, has emerged. These structures are implemented using judicious manipulation of loss and gain mechanisms<sup>9-21</sup>. Their spectra undergo a transition from real to complex once the parameter that controls the degree of gain and loss in the system reaches a critical value<sup>22</sup>. The transition point shows the characteristic features of an *exceptional point* (EP), where both eigenfrequencies and normal modes coalesce. For values of the gain and loss parameter which are smaller than the critical value the eigenvectors of the equations of motion are also eigenvectors of the  $\mathcal{PT}$  operator while above the critical value, they cease to be eigenvectors of the  $\mathcal{PT}$  operator. The former domain is termed the *exact phase* while the latter is the *broken phase*. This terminology is borrowed from the “ $\mathcal{PT}$ -symmetric quantum mechanics” community (see the review<sup>23</sup>). One should keep in mind, though, that the systems studied in<sup>9-21</sup> are purely

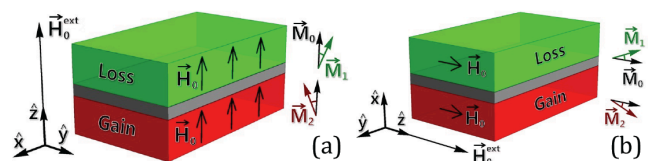


FIG. 1: Two coupled ferromagnetic films in the presence of an external magnetic field which is along the  $z$ -axis. We distinguish between two geometries: (a) Out of plane geometry (the  $z$ -axis is perpendicular to the films) and (b) In plane geometry (the  $z$ -axis is parallel to the films).

classical, with loss and gain being introduced on a phenomenological level, and as such they are quite different from the  $\mathcal{PT}$ -symmetric quantum systems envisaged by Bender and collaborators<sup>23</sup>.

The resulting wave structures show several intriguing features such as power oscillations<sup>9-13</sup>, non-reciprocity of wave propagation<sup>14-16</sup>, unidirectional invisibility<sup>11,17-19</sup> and coherent perfect absorbers and lasers<sup>20</sup> etc. Experimental realizations have been reported in the framework of optics<sup>10,11,16,17,21</sup> and electronic circuitry<sup>12,15,18</sup> while the applicability of these ideas has been theoretically demonstrated in Bose-Einstein Condensates<sup>24</sup> and in acoustics<sup>25</sup>.

In this paper we propose a class of synthetic magnetic nanostructures which utilize natural dissipation (loss) mechanisms together with judiciously balanced amplification (gain) processes in order to control magnetization dynamics. Amplification in such structures can be achieved with the help of certain external factors such as parametric driving or spin-transfer torque (see Sec. V), while loss comes from coupling with the phonons or other degrees of freedom. As a prototype system we consider two ferromagnetic films (see Fig. 1), one with loss and the other with equal amount of gain, coupled by an exchange or by a dipole-dipole interaction. The magnetization dynamics is described in terms of two vector variables, the macroscopic magnetic moments of each film, whose evo-

lution is given by the non-linear Landau-Lifshitz-Gilbert equations. We will demonstrate that despite the fact that the system is non-hermitian, if the gain and loss parameter is below a critical value, the macroscopic magnetic moments precesses about the direction of an effective magnetic field inside the sample without being amplified or attenuated. Specifically, below a critical value of the gain and loss parameter, the eigenmodes are real while above this critical value, they become complex, leading to dynamical instabilities that are limited only by non-linear effects. The transition point is characterized by an EP degeneracy. Our proposal reveals a new type of steady state dynamics which can be useful for manipulating magnetization switching and potentially lead to new device design. Moreover, the realization of EP degeneracies may be utilized for enhanced sensitivity in sensing via frequency splitting.

The structure of the paper is as follows. In the next section II we present the mathematical model that describes our system. It consists of two coupled nonlinear Landau-Lifshitz-Gilbert (LLG) equations. In section III we investigate the out-of-plane geometry. In subsection III.A we analyze the eigenfrequencies and the eigenmodes of the linearized LLG equations for different values of the gain and loss parameter. The dynamics generated by the  $\mathcal{PT}$ -symmetric LLG equations and its comparison to the results from the linearized LLG equations are discussed in subsection III.B. In section IV we analyze an in-plane (magnetization) geometry. Finally in section V we discuss two different physical mechanisms which allow us to incorporate and manage gain in a magnetic nanostructure. Our conclusions are given in section VI.

## II. MATHEMATICAL MODELING

We consider two ferromagnetic films  $n = 1, 2$  separated by a non-magnetic layer. The two geometries that we will consider here are shown in Fig. 1. In Fig. 1a, we assume a uniform external magnetic field  $\vec{H}_{\text{ext}}$  perpendicular to the plane of the films (out of plane geometry) while in Fig. 1b the external field is parallel to the films (in-plane geometry). The magnetization within each film is uniform and is represented by a magnetic vector  $\vec{M}_{n=1,2}$ . When the magnetic configuration is away from equilibrium the magnetization precesses around the instantaneous local effective field  $\vec{H}_n$ . The latter is generally a complicated function of  $\vec{M}_n$  and the external magnetic field  $\vec{H}_{\text{ext}}$ . For the cases shown in Fig. 1 we have

$$\vec{H}_n = \vec{H}_{\text{ext}} - 4\pi\hat{N}\vec{M}_n \quad (1)$$

where the demagnetizing tensor  $\hat{N}$  takes the simple form  $\hat{N}_{i,j} = \delta_{i,3}\delta_{j,3}$  for the out of plane geometry and  $\hat{N}_{i,j} = \delta_{i,1}\delta_{j,1}$  for the in-plane geometry ( $i, j = 1, 2, 3$  indicates the  $\hat{x}, \hat{y}, \hat{z}$  directions respectively).

The time-evolution of the magnetization dynamics for this coupled system can be described by a pair of coupled

modified Landau-Lifshitz-Gilbert (LLG):

$$\begin{aligned} \frac{\partial \vec{M}_1}{\partial t} &= -\gamma \vec{M}_1 \times \vec{H}_1 - \gamma K \vec{M}_1 \times \vec{M}_2 + \frac{\alpha}{|\vec{M}_1|} \vec{M}_1 \times \frac{\partial \vec{M}_1}{\partial t} \\ \frac{\partial \vec{M}_2}{\partial t} &= -\gamma \vec{M}_2 \times \vec{H}_2 - \gamma K \vec{M}_2 \times \vec{M}_1 - \frac{\alpha}{|\vec{M}_2|} \vec{M}_2 \times \frac{\partial \vec{M}_2}{\partial t} \end{aligned} \quad (2)$$

where  $\gamma$  is the gyromagnetic ratio. The first term on the right-hand sides of Eqs. (2) describes the interaction of the magnetization  $\vec{M}_n$  of each layer with the corresponding local field  $\vec{H}_n$ . The second term represents the coupling between the two ferromagnetic layers. We assume ferromagnetic coupling i.e.  $K > 0$ . The last term of the first equation describes dissipation processes and can be introduced in the original LLG equations by assuming that an effective local friction is pushing the magnetic moment  $\vec{M}_1$  towards the direction of the effective magnetic field acting on that moment. It was introduced by Gilbert in order to describe dissipation and can be shown to be equivalent to the term that was proposed originally by Landau and Lifshitz for the same purpose<sup>1</sup>. The parameter  $\alpha$  is the Gilbert damping term. The last term of the second equation is similar but the sign is reversed, reflecting the possibility of amplification mechanisms. We discuss experimentally realizable ways to achieve "gain" at the last section V of this paper.

For  $\alpha = 0$ , Eqs. (2) are invariant with respect to the interchange  $\vec{M}_1 \leftrightarrow \vec{M}_2$ . Notice that this interchange implies also an interchange of  $\vec{H}_1 \leftrightarrow \vec{H}_2$  via Eq. (1). We refer to this symmetry as the "parity" ( $\mathcal{P}$ ) symmetry. When  $\alpha \neq 0$  the parity symmetry of our system is destroyed. However, Eqs. (2) are still invariant under a *combined* parity  $\mathcal{P}$  and time reversal  $\mathcal{T}$  operations. The latter corresponds to a time inversion  $t \rightarrow -t$  together with a simultaneous change of the sign of all pseudovectors i.e.  $\vec{M}_n \rightarrow -\vec{M}_n$  and  $\vec{H}_n \rightarrow -\vec{H}_n$ . This definition of the time reversal operation is necessary when magnetic fields, which break the time reversibility in a Hermitian manner, are present. Finally we note that all terms in Eqs. (2) conserve the length of the magnetization vectors  $\vec{M}_n$ . This can be easily seen by taking the inner product of each of the above equations with the respective  $\vec{M}_n$ . This yields  $\vec{M}_n \cdot \frac{\partial \vec{M}_n}{\partial t} = \frac{1}{2} \frac{\partial \vec{M}_n^2}{\partial t} = 0$ , indicating that  $|\vec{M}_n|$  are constants of motion.

Below, we first analyze the parametric evolution of the eigenfrequencies and normal modes associated with small oscillations around the equilibrium configuration as the gain and loss parameter  $\alpha$  increases. To this end, we separate the magnetization of each film into its equilibrium value which is assumed to be the same for both films,  $\vec{M}_n^{(0)} = \vec{M}^{(0)}$ , and its oscillating part  $\vec{m}_n$  i.e.  $\vec{M}_n = \vec{M}^{(0)} + \vec{m}_n$  where  $|\vec{m}_n| \ll |\vec{M}^{(0)}|$ . Furthermore, the external magnetic field can be decomposed into its constant value  $\vec{H}_{\text{ext}}^{(0)}$  and a time-dependent part  $\vec{h}_{\text{ext}}$  i.e.  $\vec{H}_{\text{ext}} = \vec{H}_{\text{ext}}^{(0)} + \vec{h}_{\text{ext}}$ . In the next section III we focus on

the out of plane geometry (see Fig. 1a) while at section IV we briefly discuss the in-plane geometry (see Fig. 1b).

### III. OUT OF PLANE GEOMETRY

#### A. Linearized LLG Equations and Parametric Evolution of its Normal Modes

For the out of plane geometry we recall the relation (1) which allows us to connect the external field  $\vec{H}_{\text{ext}}$  to the local internal field  $\vec{H}_n$ . Linearizing Eq. (2) with respect to  $\vec{m}_n$  and, furthermore, setting  $\vec{h}_{\text{ext}} = 0$  we obtain the following linear set of equations

$$\begin{aligned} \frac{\partial \vec{m}_1}{\partial t} &= (\omega_H + \omega_K) \hat{z} \times \vec{m}_1 - \omega_K \hat{z} \times \vec{m}_2 + \alpha \hat{z} \times \frac{\partial \vec{m}_1}{\partial t} \\ \frac{\partial \vec{m}_2}{\partial t} &= (\omega_H + \omega_K) \hat{z} \times \vec{m}_2 - \omega_K \hat{z} \times \vec{m}_1 - \alpha \hat{z} \times \frac{\partial \vec{m}_2}{\partial t} \end{aligned} \quad (3)$$

where  $\omega_K = \gamma K |\vec{M}_0|$  and  $\omega_H = \gamma |\vec{H}_0|$ . Here  $|\vec{H}_0| = |\vec{H}_{\text{ext}}^{(0)} - 4\pi |\vec{M}_0|$  is the constant internal magnetic field which is assumed to be the same for both films.

Assuming a harmonic time-dependence for the magnetization  $\vec{m}_n(t) = \vec{m}_n \exp(-i\omega t)$ , we have

$$\begin{aligned} -i\omega \vec{m}_1 &= (\omega_H + \omega_K - i\alpha\omega) \hat{z} \times \vec{m}_1 - \omega_K \hat{z} \times \vec{m}_2 \\ -i\omega \vec{m}_2 &= (\omega_H + \omega_K + i\alpha\omega) \hat{z} \times \vec{m}_2 - \omega_K \hat{z} \times \vec{m}_1 \end{aligned} \quad (4)$$

Note that, although formally  $\vec{m}_1$  and  $\vec{m}_2$  are three-dimensional vectors, only the transverse ( $x, y$ ) components appear in a non-trivial manner. The longitudinal components  $m_{1z}$  and  $m_{2z}$  are zero in the linear approximation, as follows from Eqs. (4). This is a straightforward consequence of the already mentioned constraint of the strictly conserved length of vectors  $\vec{M}_1$  and  $\vec{M}_2$ . Thus, the magnetic vectors have only two independent components and, if the transverse components are known, the longitudinal component can be found from the constraint. When  $\vec{m}_1$  is treated in the linear approximation, then  $m_{1z} = -m_1^2/2|\vec{M}_1^{(0)}|$  (and similarly for  $m_{2z}$ ). In subsection IIIB, where the exact nonlinear dynamics is treated, we use spherical coordinates which makes it manifestly clear that there are only two independent degrees of freedom (two angles) for each magnetic moment.

The analysis of Eq. (4) can be simplified by using the “center of mass” coordinates of the system. We define  $\vec{\Delta} \equiv \vec{m}_1 - \vec{m}_2$  and  $\vec{\mu} \equiv \vec{m}_1 + \vec{m}_2$ . Then Eqs. (4) take the following form:

$$\begin{aligned} [(1 + \alpha^2)\omega^2 - (\omega_H + 2\omega_K)^2] \vec{\Delta} + 2i\alpha\omega(\omega_H + \omega_K)\vec{\mu} &= 0 \\ 2i\alpha\omega(\omega_H + \omega_K)\vec{\Delta} + [(1 + \alpha^2)\omega^2 - \omega_H^2] \vec{\mu} &= 0 \end{aligned} \quad (5)$$

which allows us to decouple the  $x$  and  $y$  components of the center of mass coordinates  $\vec{\Delta}, \vec{\mu}$ . Thus the original

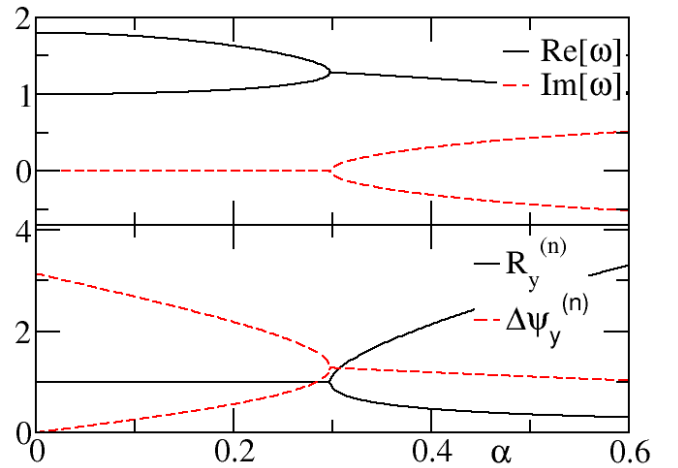


FIG. 2: (Up) Parametric evolution of the eigen-frequencies of a  $\mathcal{PT}$ -symmetric ferromagnetic dimer shown in Fig. 1a. The parameters used are such that  $\omega_K = 0.4\omega_H$ . (Down) The same but now for the magnitude of the ratio between the  $y$ -components of the normal modes and their associated phase difference. The same behaviour holds also for the  $x$ -components.

set of four coupled equations reduces to two uncoupled sets for the  $x$  and  $y$  components respectively.

The eigenvalues and the normal modes can be found by solving the  $2 \times 2$  secular equation for one of these components. The eigenfrequencies are given by:

$$\omega_{1,2} = \frac{\omega_H + \omega_K \pm \sqrt{\omega_K^2 - \alpha^2\omega_H(\omega_H + 2\omega_K)}}{1 + \alpha^2} \quad (6)$$

The limiting case of  $\alpha = 0$  results in two eigenfrequencies: (a)  $\omega_1 = \omega_H$  associated with the “soft” mode (frequency approaches zero when  $|\vec{H}_0| \rightarrow 0$ ), with  $\vec{m}_1 = \vec{m}_2$  and (b)  $\omega_2 = \omega_H + 2\omega_K$  associated with the “hard” mode, with  $\vec{m}_1 = -\vec{m}_2$ . As the gain and loss parameter  $\alpha$  increases the two eigenfrequencies approach one another (see Fig. 2) and at some critical value  $\alpha = \alpha_{\text{cr}}$  they coalesce and bifurcate into the complex plane. Using Eq. (6) we calculate the critical frequency  $\omega_{\text{cr}}$  and the critical value of gain and loss parameter to be

$$\alpha_{\text{cr}} = \frac{\omega_K}{\sqrt{\omega_H(\omega_H + 2\omega_K)}}, \quad \omega_{\text{cr}} = \frac{\omega_H(\omega_H + 2\omega_K)}{\omega_H + \omega_K} \quad (7)$$

Near the phase transition point  $\alpha_{\text{cr}}$ , the eigenfrequencies display the characteristic behavior of an exceptional point  $|\omega| \propto \sqrt{\alpha - \alpha_{\text{cr}}}$ . This behavior can be exploited in sensing technologies since it enhances the sensitivity of frequency splitting detection (for an optics proposal see Ref<sup>26</sup>).

Next we evaluate the normal modes of the ferromagnetic dimer. Using Eqs. (5,6) we first evaluate  $\vec{\Delta}, \vec{\mu}$  and

from there extract the original variables  $\vec{m}_n$ . This yields

$$\begin{pmatrix} m_{1x}^{(l)} \\ m_{1y}^{(l)} \\ m_{2x}^{(l)} \\ m_{2y}^{(l)} \end{pmatrix} = \begin{pmatrix} \frac{\alpha(\omega_H + \omega_K) \pm i\sqrt{\omega_K^2 - \alpha^2\omega_H(\omega_H + 2\omega_K)}}{(1+i\alpha)\omega_K} \\ i\frac{(\alpha(\omega_H + \omega_K) \pm i\sqrt{\omega_K^2 - \alpha^2\omega_H(\omega_H + 2\omega_K)})}{(1+i\alpha)\omega_K} \\ -i \\ 1 \end{pmatrix} \quad (8)$$

where the sub-indexes  $x, y$  refer to the  $x, y$  components of the magnetization vectors and the super-index  $l = 1, 2$  refers to the normal mode corresponding to  $+, -$  signs at the rhs of Eq. (8) respectively.  $\mathcal{PT}$ -symmetry considerations require that in the exact phase, in contrast to the broken one, these vectors are also eigenvectors of the  $\mathcal{PT}$ -operator. In other words, the ratio of the magnitudes of the relevant components  $R_x^{(l)} \equiv \left| \frac{m_{1x}^{(l)}}{m_{2x}^{(l)}} \right|$ ;  $R_y^{(l)} \equiv \left| \frac{m_{1y}^{(l)}}{m_{2y}^{(l)}} \right|$  in the exact phase is unity indicating that the magnitude of the magnetization eigenvectors is the same in both the loss and the gain side of the dimer. As  $\alpha$  becomes larger than  $\alpha_{\text{cr}}$  the magnitude of the magnetization in the loss and in the gain sides become unequal indicating that the magnetization eigenmodes reside either on the gain or the lossy side of the dimer. This behavior can be seen nicely in Fig. 2b where we are plotting  $R_y^{(l=1,2)}$  as well as the relative phase difference  $\Delta\psi_y^{(l=1,2)}$  between the  $y$  components of the  $l = 1, 2$  modes. We see that for  $\alpha = 0$  the phase difference assumes the values  $\Delta\psi_y^{(l=1)} = 0$  and  $\Delta\psi_y^{(l=2)} = \pi$  indicating a symmetric ( $\vec{m}_1 = \vec{m}_2$  corresponding to the soft mode) and anti-symmetric ( $\vec{m}_1 = -\vec{m}_2$  corresponding to the hard mode) combinations. At  $\alpha = \alpha_{\text{cr}}$  we have a degeneracy of the eigenvectors.

## B. Nonlinear Time Evolution

The  $\mathcal{PT}$ -symmetric nature of the dimer is also encoded in the time evolution of the magnetization vectors and the realization of new types of steady-states. The precession dynamics is better represented in spherical coordinates i.e. switching to the angular variables  $\Theta_{1,2}$  and  $\Phi_{1,2}$

$$\begin{aligned} M_{nx} &= M_0 \sin(\Theta_n) \cos(\Phi_n); \\ M_{ny} &= M_0 \sin(\Theta_n) \sin(\Phi_n); \\ M_{nz} &= M_0 \cos(\Theta_n) \end{aligned} \quad (9)$$

These variables are particularly convenient for studying the dynamics because they unveil the fact that there are only two (and not three) independent dynamical variables for each magnetic moment. Specifically we concentrate on the temporal evolution of the polar angles  $\Theta_n(t)$ , with respect to the direction of the internal magnetic fields  $\vec{H}_n$  ( $z$ -direction). These polar angles are related to the  $z$ -components of the magnetic moments. The dynamics of the transverse components is less interesting (just a rapid precession) and it is encoded in the azimuthal angle  $\Phi_n$ .

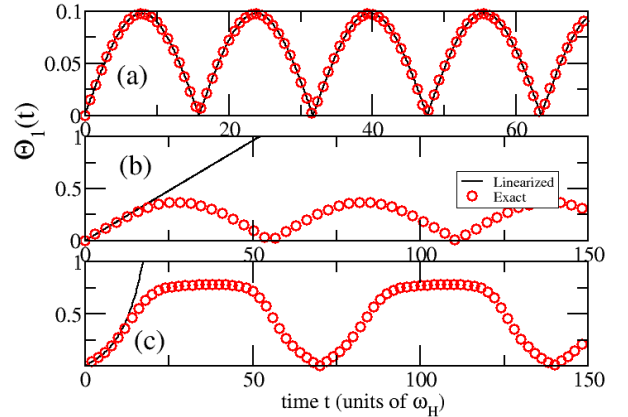


FIG. 3: Time dependence of the polar angle  $\Theta_1(t)$  associated with the magnetization vector of lossy film. The initial conditions in all cases are  $\Theta_1(t=0) = 0 = \Phi_1(t=0)$  and  $\Theta_2(t=0) = 0.05, \Phi_2(t=0) = \pi/2$  while  $\omega_K = 0.4\omega_H$ . The results of the exact dynamics Eq. (2) are indicated with red circles while the dynamics generated by the linearized Eqs (3) are indicated with a black line. (a) Exact phase for  $\alpha = 0.85\alpha_{\text{cr}}$ ; (b) Dynamics at the exceptional point i.e.  $\alpha = \alpha_{\text{cr}}$ ; (c) Broken phase with  $\alpha = 1.1\alpha_{\text{cr}}$ . Time is measured in units of inverse  $\omega_H$ .

In the case of a single film, where only dissipative mechanisms are taken into account,  $\Theta_n$  decreases due to energy losses so that the magnetization vectors align with the  $\hat{z}$ -direction. Conversely, in the presence of amplification mechanisms only, the magnetization of a single film is driven away from the  $\hat{z}$ -direction.

In the case of  $\mathcal{PT}$ -symmetric configurations, where a dissipative and an amplified film are coupled together, the resulting dynamics depends on the value of the gain and loss parameter  $\alpha$ . Below we present exact numerical solutions of Eqs. (2), for various cases.

When  $\alpha < \alpha_{\text{cr}}$  (exact phase, see Fig. 3a and Fig. 4a), despite the fact that the dimer is non-Hermitian, the polar angles  $\Theta_n$  oscillate around the initial misalignment from the  $\hat{z}$ -axis without being amplified or attenuated, indicating the existence of a new type of steady state. In this domain the linearized equations (3) describe well the exact dynamics (2).

In the broken phase  $\alpha > \alpha_{\text{cr}}$  (see Fig. 3c and Fig. 4c), the evolution generated by the linearized equations (3) indicates an exponential growth of  $\Theta_n$  (black lines in Figs. 3c and 4c) which is associated with the fact that the eigenfrequencies are acquiring an imaginary part. In other words, in this domain, the linear solution is unstable and the linear approximation is inadequate to describe the dynamics. This exponential growth is eventually suppressed by non-linear effects which are inherent in the original LLG equations (2). A (numerically exact) solution of the nonlinear problem, for  $\Theta_1$  as a function of time, is shown in Fig. 3c by red circles (a similar be-

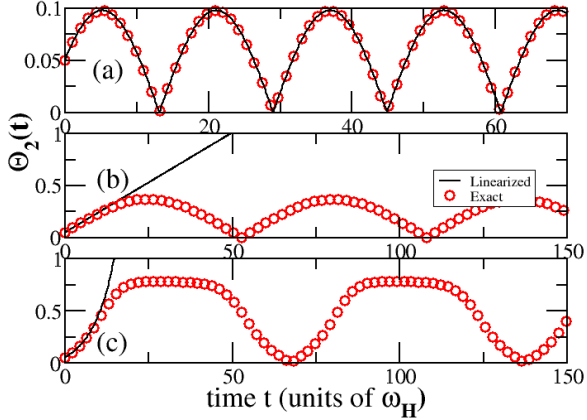


FIG. 4: Time dependence of the polar angle  $\Theta_2(t)$  associated with the magnetization vector of “gain” film. The initial conditions and parameters are the same as the one used in Fig. 3. Time is measured in units of inverse  $\omega_H$ .

havior is observed for  $\Theta_2$ ; see Fig. 4c). This solution corresponds to the initial conditions  $\Theta_1(t=0) = 0 = \Phi_1(t=0)$ ,  $\Theta_2(t=0) = 0.05$ , and  $\Phi_2(t=0) = \pi/2$  and it is periodic in time. We have checked that the period slightly depends on the choice of the initial conditions. In all cases, however, we find a stable periodic solution with no sign of any “run away” effects.

Similar behavior is observed at the transition point corresponding to  $\alpha = \alpha_{cr}$ , with the alteration that the linearized equations (3) lead to a linear growth of the polar angles  $\Theta_n$  (see Fig. 3b and Fig. 4b). This behavior is a consequence of the EP degeneracy which results in defective eigenmodes. The particular solution in Fig. 3b and Fig. 4b correspond to the initial conditions  $\Theta_1(t=0) = 0 = \Phi_1(t=0)$  and  $\Theta_2(t=0) = 0.05$ ,  $\Phi_2(t=0) = \pi/2$ . We conclude therefore that the linear approximation, which is applicable only in the case for which  $\Theta_n \ll 1$ , fails to describe the actual dynamics when  $\alpha = \alpha_{cr}$ .

Finally, we point out that we have checked numerically that the behavior of the angular variables  $\Theta_{1,2}$  as discussed above and shown in Figs. 3,4 is typical and it is qualitatively the same for other choices of initial conditions.

#### IV. IN-PLANE GEOMETRY

For completeness of our study we also analyze the in-plane geometry shown in Fig. 1b. Following the same program as previously we can linearize the LLG equations (under the condition  $\vec{h}_{ext} = 0$ ) and study the dynamics of magnetization vectors  $\vec{m}_n$ . For this geometry the equations for  $\vec{m}_n$  differ from Eq. (3) by an additional term  $\omega_M m_{nx} \hat{y}$  on the right hand side where

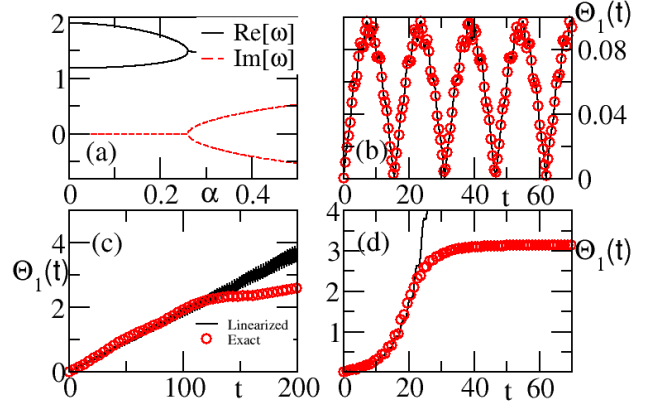


FIG. 5: In an in-plane geometry (Fig. 1b) for  $\omega_K = 0.4\omega_H$  and  $\omega_M = 0.4\omega_H$ : (a) The parametric evolution of eigenfrequencies versus the gain-loss parameter  $\alpha$ ; The temporal evolution of  $\Theta_1(t)$  in the (b) exact phase with  $\alpha = 0.85\alpha_{cr}$ ; (c) EP with  $\alpha = \alpha_{cr}$  and (d) broken phase with  $\alpha = 1.1\alpha_{cr}$ . The initial condition and lines/symbols are the same as in Fig. 3. Time is measured in units of inverse  $\omega_H$ . We have used the same initial conditions as the one used in Fig. 3.

$$\omega_M = 4\pi\gamma M_0:$$

$$\begin{aligned} \frac{d\vec{m}_1}{dt} &= (\omega_H + \omega_K)\hat{z} \times \vec{m}_1 - \omega_K \hat{z} \times \vec{m}_2 + \\ &\quad \omega_M m_{1x} \hat{y} + \alpha \hat{z} \times \frac{d\vec{m}_1}{dt} \\ \frac{d\vec{m}_2}{dt} &= (\omega_H + \omega_K)\hat{z} \times \vec{m}_2 - \omega_K \hat{z} \times \vec{m}_1 + \\ &\quad \omega_M m_{2x} \hat{y} - \alpha \hat{z} \times \frac{d\vec{m}_2}{dt} \end{aligned} \quad (10)$$

These equations enable one to calculate the normal modes of the system as well as the linear dynamics. We have also obtained a solution of the full nonlinear problem for the in-plane geometry. Some representative results are reported in Fig. 5 showing a behavior qualitatively similar to that for the out of plane configuration.

## V. REALIZATION OF GAIN IN FERROMAGNETIC LAYERS

In this section we would like to point out two possible ways to achieve amplification (gain) of the magnetic oscillations in ferromagnets.

### A. Parametric driving

Let us first recall the phenomenon of the parametric resonance of a harmonic oscillator<sup>27</sup>. Consider an oscillator whose eigenfrequency is modulated in time so that

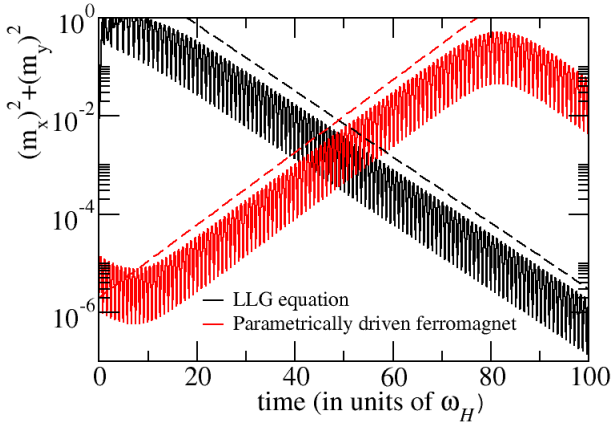


FIG. 6: The temporal behavior of the magnetization  $m_x^2 + m_y^2$  of a dissipative (black line) and an amplified (red) ferromagnet where gain is introduced via parametric driving. The driving parameters in the last case are such that the amplification increment has equal magnitude, but opposite sign, with respect to the lossy ferromagnet. The dashed lines are drawn in order to guide the eye and indicate that the ratios in these two cases are the same. The time is measured in units of inverse  $\omega_H$ .

the equation of motion is

$$\ddot{x}(t) + \omega_0^2 [1 + \eta \cos(2\omega_0 t)] x(t) = 0; \quad (\eta \ll 1) \quad (11)$$

The approximate solution of this equation is

$$x(t) = a(t) \sin(\omega_0 t) + b(t) \cos(\omega_0 t) \quad (12)$$

where the slowly varying amplitudes  $a(t), b(t)$  grow exponentially with time, with an increment  $(\eta\omega_0/4) = \lambda \ll \omega_0$ . Thus, the parametrically driven oscillator exhibits an instability (gain). The equilibrium solution  $x(t) = 0$  of Eq. (11) is unstable, i.e. an infinitesimal deviation from equilibrium results in an exponential growth. This growth, on top of rapid oscillations with frequency  $\omega_0$ , can be modeled by the equation

$$\ddot{x}(t) - 2\lambda\dot{x}(t) + \omega_0^2 x(t) = 0. \quad (13)$$

This exponential growth  $\exp(\lambda t)$ , is eventually limited by non-linear effects.

A similar phenomenon occurs for a magnetic moment driven by an appropriate external magnetic field. Consider the in-plane geometry with the external field

$$\vec{H}_{\text{ext}} = [H_{\text{ext}}^{(0)} + h_{\text{ext}}(t)] \hat{z} \quad (14)$$

in the  $\hat{z}$ -direction (in the plane of the film), where the weak, time-dependent component can be written as  $H_{\text{ext}}^{(0)} \eta f(t)$ . The geometry when the dc and ac external fields are parallel to one another is known as longitudinal (or parallel) pumping. Such pumping can lead to excitation of spin waves, with a wavelength smaller than the

size of the sample<sup>28</sup>. We, however, are interested only in the uniform magnetization of the entire sample.

Since  $\vec{h}_{\text{ext}}$  is in the same direction as  $H_{\text{ext}}^{(0)}$  (which is also in the direction of the equilibrium magnetization  $\vec{M}_0$ ) it cannot cause the ordinary precession of the magnetic moment about the  $\hat{z}$ -direction. Rather, it can cause an instability via a mechanism analogous to the parametric driving of a harmonic oscillator (see Fig. 6). Indeed, neglecting for the moment the losses, the linearized Landau-Lifshitz equations read:

$$\begin{aligned} \dot{m}_x &= -\omega_H [1 + \eta f(t)] m_y \\ \dot{m}_y &= \omega_H [1 + \eta f(t)] m_x + \omega_M m_x \end{aligned} \quad (15)$$

where  $\omega_H = \gamma H_0$ ,  $\omega_M = 4\pi\gamma M_0$ . (Recall that in this geometry the internal field  $H_0 = H_{\text{ext}}^{(0)}$ ). We do not pursue the detail analysis of Eq. (15) but only notice that for the case  $\omega_M \gg \omega_H$  the second of the Eqs. (15) reduces to  $\dot{m}_y = \omega_M m_x$  which, after taking a time derivative and substituting  $\dot{m}_x$  from the first Eq. (15), yields  $\ddot{m}_y = -\omega_H \omega_M [1 + \eta f(t)] m_y$ . For  $f(t) = \cos(2\omega_0 t)$ , with  $\omega_0 = \sqrt{\omega_H \omega_M}$ , this coincides with Eq. (11) for the parametrically driven oscillator. Thus a magnetic moment, parametrically driven with an ac magnetic field, parallel to the constant field Eq. (14), exhibits an instability, i.e. an exponential growth of the precession angle  $\Theta$  about the  $\hat{z}$ -direction, limited only by nonlinearity. Such an instability is modeled by reversing the sign of the attenuation term in the Landau-Lifshitz (Gilbert) equation.

Finally, the analysis can be extended to include a decay term into the Landau-Lifshitz equations, in a way similar to the inclusion of a weak friction into Eq. (11) for the oscillator<sup>27</sup> (see Fig. 6).

## B. Spin transfer torque

A different mechanism for achieving amplification of the magnetic moment precession is based on the spin transfer phenomenon (see Ref.<sup>29</sup> for a pedagogical review). When spin-polarized electrons are scattered on a ferro-magnetic layer, they generally transfer some angular momentum to the layer, thus inducing a torque  $\vec{N}$  on the magnetic moment  $\vec{M}$ , see Fig. 7. (Spin polarization is usually achieved by passing current through another ferromagnetic layer - a "spin polarizer" - not shown in the figure). Two conditions should be satisfied for the spin transfer to take place: First, the scattering amplitudes must be spin-dependent, i.e. be different for spin-up (parallel to  $\vec{M}$ ) and spin-down electrons (such difference is provided by the exchange splitting between the minority and majority spin-bands in the ferromagnet). Second, polarization direction of the incident spins  $\vec{S}$ , should not be strictly parallel to the direction of  $\vec{M}$ . The angular momentum, transmitted to the ferro-magnetic layer by the stream of polarized electrons, affects the dynamics of the magnetic moment  $\vec{M}$ . The effect is described by an

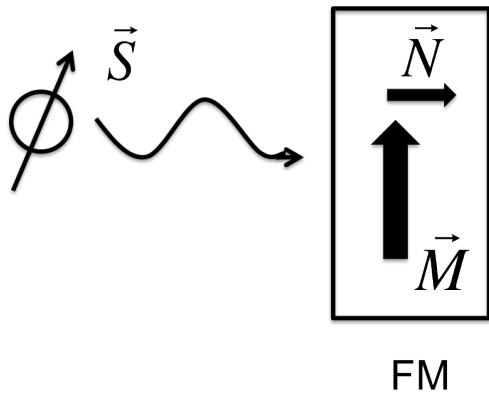


FIG. 7: A beam of spin-polarized electrons impinges on a ferro-magnetic layer (FM) with magnetic moment  $\vec{M}$ .

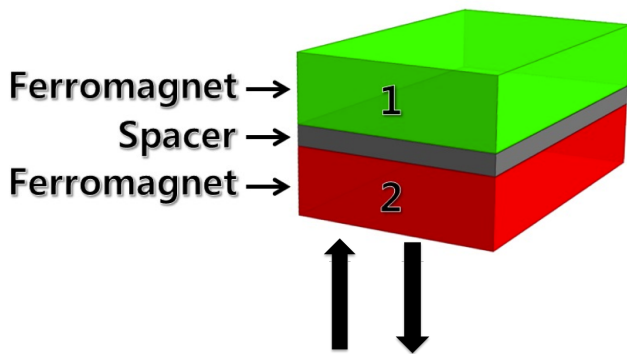


FIG. 8: Spin-polarized electrons (up-pointing arrow) impinges on the ferromagnetic layer and are reflected back (down-pointing arrow). Spin angular momentum (but no electric current!) is flowing into the layer, creating gain. The red layer indicate the gain ferromagnet while the green layer indicate the lossy ferromagnet.

amplification term in the Landau-Lifshitz equation. This term has the same form as the damping term but with an opposite sign (the resulting equation is referred to as the Landau-Lifshitz-Gilbert-Slonczewski equation).

It is interesting to note that spin transfer can occur even in the case of total reflection, provided that the reflection amplitudes for up and down-spins,  $r_{\text{up}} = \exp(i\phi_{\text{up}})$  and  $r_{\text{down}} = \exp(i\phi_{\text{down}})$ , have different phases, see Eq. (14) in Ref.<sup>29</sup>. Although the "transmitted" wave in this case is purely evanescent, so that no charge current can flow into the layer, the angular momentum transmitted to the layer is not zero<sup>29,30</sup>. This might provide the most practical way for producing gain in a  $\mathcal{PT}$ -symmetric magnetic structure, see Fig. 8. Again, as in Fig. 7, we do not show explicitly the set-up which produces the spin-polarized current that impinges on the lower film (gain) of our  $\mathcal{PT}$ -symmetric device. One can find the full set-up in Ref.<sup>30</sup>.

## VI. CONCLUSIONS

In conclusion, we have introduced the notion of  $\mathcal{PT}$ -symmetry in magnetic nanostructures. Using two coupled ferromagnetic layers, one with loss and another with equal amount of gain, we demonstrated the emergence of a new type of steady-state dynamics where the polar angle, although not a constant of motion, is bounded and neither attenuates (as in the case of losses) nor amplifies (as in the case of gain). This non-Hermitian steady state can be reached for values of the gain and loss parameter  $\alpha$  that are below a critical value  $\alpha_{\text{cr}}$ . At  $\alpha = \alpha_{\text{cr}}$  the system experiences an exceptional point degeneracy where both eigenvalues and eigenvectors are simultaneously degenerate. It will be interesting to extend this study to the case of spin waves (magnons) and investigate the possibility of observing phenomena such as magnonic Coherent Perfect Absorbers/Lasing, invisibility etc<sup>19,20</sup>.

## Acknowledgments

We are grateful to V. Vardeny for attracting our interest to the subject. This research was partially supported by an AFOSR MURI grant FA9550-14-1-0037 and by an NSF ECCS-1128571 and DMR-1306984 grants. (B.S) acknowledges a Global Initiative grant from Wesleyan University (Dean's office).

<sup>1</sup> D. D. Stancil, A. Prabhakar, *Spin Waves: Theory and Applications*, Springer (2009).

<sup>2</sup> J. Akerman, *Science* **308**, 508 (2005); S. Datta, B. Das, *Appl. Phys. Lett.* **56**, 665 (1990);

<sup>3</sup> C. D. Stanciu, F. Hansteen, A. V. Kirilyuk, A. Tsukamoto, A. Itoh, T. Rasing, *Phys. Rev. Lett.* **99**, 047601 (2007); J. Stöhr, H. C. Siegmann, A. Kashuba, S. J. Gamble, *Appl. Phys. Lett.* **94**, 072504 (2009).

<sup>4</sup> A. V. Nazarov, H. S. Cho, J. Nowak, S. Stokes, N. Tabat, *Appl. Phys. Lett.* **81**, 4559 (2002); S. Ghionea, P. Dhagat, A. Jander, *IEEE Sensors Journal* **8**, 1530 (2008).

<sup>5</sup> D. C. Ralph, M. D. Stiles, *J. Magn. Magn. Mater.* **320**,

1190 (2008); J. A. Katine, E. E. Fullerton, *J. Magn. Magn. Mater.*, **320**, 1217 (2008).

<sup>6</sup> N. Engheta and R. W. Ziolkowski, *Metamaterials: Physics and Engineering Explorations*, John Wiley & Sons & IEEE Press (2006); L. Solymar, E. Shamonina, *Waves in Metamaterials*, Oxford University Press, USA (2009).

<sup>7</sup> C. Caloz, T. Itoh, *Electromagnetic Metamaterials: Transmission Line Theory and Microwave Applications*, Wiley (2006)

<sup>8</sup> P. Deymier, *Acoustic Metamaterials and Phononic Crystals*, Springer Series in Solid-State Sciences **173** (2013).

<sup>9</sup> K. G. Makris, R. El-Ganainy, D. N. Christodoulides and

- Z. H. Musslimani, Phys. Rev. Lett. **100**, 103904 (2008); Z. H. Musslimani, K. G. Makris, R. El-Ganainy, and D. N. Christodoulides, Phys. Rev. Lett. **100**, 030402 (2008).
- <sup>10</sup> C. Ruter, K. Makris, R. El-Ganainy, D. Christodoulides, M. Segev, and D. Kip, Nat. Phys. **6**, 192 (2010).
- <sup>11</sup> A. Regensburger, C. Bersch, M.-A. Miri, G. Onishchukov, D. N. Christodoulides, and Ulf Peschel, Nature (London) **488**, 167 (2012).
- <sup>12</sup> J. Schindler, Z. Lin, J. M. Lee, H. Ramezani, F. M. Ellis, T. Kottos, J. Phys. A: Math. Theor. **45**, 444029 (2012); H. Ramezani, J. Schindler, F.M. Ellis, U. Gunther, and T. Kottos, Phys. Rev. A **85**, 062122 (2012)
- <sup>13</sup> M.C. Zheng, D.N. Christodoulides, R. Fleischmann, and T. Kottos, Phys. Rev. A **82**, 010103 (2010).
- <sup>14</sup> H. Ramezani, T. Kottos, R. El-Ganainy, D. N. Christodoulides, Phys. Rev. A **82**, 043803 (2010); F. Nazari, N. Bender, H. Ramezani, M. K.Moravvej- Farshi, D. N. Christodoulides, and T. Kottos, Opt. Express **22**, 9575 (2014).
- <sup>15</sup> N. Bender, S. Factor, J. D. Bodyfelt, H. Ramezani, D. N. Christodoulides, F. M. Ellis, and T. Kottos Phys. Rev. Lett. **110**, 234101 (2013)
- <sup>16</sup> B. Peng, S. K. Ozdemir, F. Lei, F. Monifi, M. Gianfreda, G. L. Long, S. Fan, F. Nori, C.M. Bender, and L. Yang, Nat. Phys. **10**, 394 (2014).
- <sup>17</sup> L. Feng, Y.-L. Xu, W. S. Fegadolli, M.-H. Lu, J. E. B. Oliveira, V. R. Almeida, Y.-F. Chen, and A. Scherer, Nat. Mater. **12**, 108 (2013).
- <sup>18</sup> Z. Lin, J. Schindler, F. M. Ellis, T. Kottos, Phys. Rev. A **85**, 050101 (2012).
- <sup>19</sup> Z. Lin, H. Ramezani, T. Eichelkraut, T. Kottos, H. Cao, D. N. Christodoulides, Phys. Rev. Lett **106**, 213901 (2011)
- <sup>20</sup> S. Longhi, Phys. Rev. A **82**, 031801 (2010); Y. D. Chong, L. Ge, A. D. Stone, Phys. Rev. Lett. **106**, 093902 (2011)
- <sup>21</sup> A. Guo, G. J. Salamo, D. Duchesne, R. Morandotti, M. Volatier-Ravat, V. Aimez, G. A. Siviloglou, and D. N. Christodoulides, Phys. Rev. Lett. **103**, 093902 (2009)
- <sup>22</sup> In the most general case, as the control parameter increases, the system can experience multiple "phase-transitions" where the spectrum changes from real to complex.
- <sup>23</sup> C. M. Bender, Rep. Prog. Phys. **70**, 947 (2007).
- <sup>24</sup> E. M. Graefe, H. J. Korsch, A. E. Niederle, Phys. Rev. Lett. **101**, 150408 (2008); M. Hiller, T. Kottos, A. Ossipov, Phys. Rev. A **73**, 063625 (2006); M. K. Oberthaler, R. Abfalterer, S. Bernet, J. Schmiedmayer, A. Zeilinger, Phys. Rev. Lett. **77**, 4980 (1996).
- <sup>25</sup> X. Zhu, H. Ramezani, C. Shi, J. Zhu, X. Zhang, Phys. Rev. X **4**, 031042 (2014); R. Fleury, D. Sounas, A. Alu, Nat. Comm. **6**, 5905 (2015).
- <sup>26</sup> J. Wiersig, Phys. Rev. Lett. **112**, 203901 (2014).
- <sup>27</sup> L. D. Landau, E. M. Lifshitz, *Mechanics*, Third Edition: Volume 1 (Course of Theoretical Physics) Pergamon Press (1976).
- <sup>28</sup> A. G. Gurevich, G. A. Melkov, *Magnetization Oscillations and Waves*, CRC Press (1996)
- <sup>29</sup> D. C. Ralph and M. D. Stiles, arXiv:0711.4608v3
- <sup>30</sup> K. Xia, P. J. Kelly, G. E. W. Bauer, A. Brataas, I. Turek, Phys. Rev. B **65**, 220401(R) (2002).